Neuron, Vol. 42, 889–896, June 24, 2004, Copyright ©2004 by Cell Press

Multiple Roles for the Active Zone Protein RIM1α in Late Stages of Neurotransmitter Release

Report

Nicole Calakos,[1] Susanne Schoch,[2,3] Thomas C. Südhof,[2] and Robert C. Malenka[1,*]
[1]Nancy Pritzker Laboratory
Department of Psychiatry and Behavioral Sciences
Stanford University School of Medicine
Palo Alto, California 94304
[2]Center for Basic Neuroscience
Department of Molecular Genetics
Howard Hughes Medical Institute
University of Texas Southwestern Medical Center
Dallas, Texas 75390

Summary

The active zone protein RIM1α interacts with multiple active zone and synaptic vesicle proteins and is implicated in short- and long-term synaptic plasticity, but it is unclear how RIM1α's biochemical interactions translate into physiological functions. To address this question, we analyzed synaptic transmission in autaptic neurons cultured from RIM1α$^{-/-}$ mice. Deletion of RIM1α causes a large reduction in the readily releasable pool of vesicles, alters short-term plasticity, and changes the properties of evoked asynchronous release. Lack of RIM1α, however, had no effect on synapse formation, spontaneous release, overall Ca^{2+} sensitivity of release, or synaptic vesicle recycling. These results suggest that RIM1α modulates sequential steps in synaptic vesicle exocytosis through serial protein-protein interactions and that this modulation is the basis for RIM1α's role in synaptic plasticity.

Introduction

Most forms of short-term plasticity (STP) are mediated presynaptically by modifying the synaptic probability of neurotransmitter release (P_r), but little is known about the molecular mechanisms that mediate the dynamic regulation of P_r by activity. P_r can be modified by a change in either the probability of release of individual quanta or the number of releasable quanta. Previous studies have identified proteins that influence P_r in an activity-dependent manner, such as the active zone protein Munc13 (Augustin et al., 1999; Rosenmund et al., 2002) and the synaptic vesicle protein Rab3A (Geppert et al., 1997; Schlüter et al., 2004). RIM1α is a particularly interesting candidate to mediate changes in P_r during synaptic plasticity, since (1) RIM1α has different effects on plasticity depending on the synapse studied (Castillo et al., 2002; Schoch et al., 2002); (2) RIM1α contains multiple protein binding domains and interacts with proteins implicated in late stages of neurotransmitter release (Coppola et al., 2001; Hibino et al., 2002; Ko et al., 2003; Ohtsuka et al., 2002; Ozaki et al., 2000; Sun et al., 2003; Wang et al., 1997, 2000); and (3) RIM1α is localized to the presynaptic active zone, the site of vesicle docking, priming, and fusion (Wang et al., 1997).

RIM (Rab3-interacting molecule) was identified by virtue of its GTP-dependent interaction with the small GTP binding protein, Rab3A (Wang et al., 1997). Biochemical experiments show that RIM1α also binds to Munc13-1, a protein required for vesicle priming (Betz et al., 2001; Wang et al., 2001); synaptotagmin 1, a calcium sensor for fast exocytosis (Coppola et al., 2001; Schoch et al., 2002); α-Liprin, a molecule implicated in synaptogenesis in *C. elegans* and *Drosophila* (Schoch et al., 2002); ERCs (Elks, Rab6-interacting protein, CAST), active zone proteins that also function in the Golgi complex (Ohtsuka et al., 2002; Wang et al., 2002); 14-3-3 proteins (Sun et al., 2003); RIM-BPs (RIM binding proteins) (Wang et al., 2000); and indirectly through RIM-BPs with L-type calcium channels (Hibino et al., 2002). These interactions suggest that RIM1α has multiple functions, perhaps as a scaffold to localize active zone components or as an integrator of the action of a series of proteins by virtue of their simultaneous or sequential binding to RIM.

Prior work in mice (Schoch et al., 2002) and *C. elegans* (Koushika et al., 2001) led to the conclusion that RIM functions at a step following the docking of synaptic vesicles at the active zone. However, transmitter release involves several steps after vesicle docking, including vesicle priming, binding of calcium to presynaptic sensors, and finally vesicle fusion. Because of the limitations of the preparations used, it was not possible to determine which postdocking step is affected in RIM1α-deficient synapses. Furthermore, the biochemical interactions of RIM1α pose a paradox. On the one hand, Rab3 and Munc13 compete with each other for binding to the amino terminus of RIM1α (Betz et al., 2001), and both interactions appear to be physiologically relevant (Castillo et al., 1997, 2002; Schoch et al., 2002). On the other hand, synapses lacking Rab3A or Munc13-1 have different phenotypes (Augustin et al., 1999; Betz et al., 1998; Geppert et al., 1997; Rosenmund et al., 2002; Schoch et al., 2002), suggesting that these proteins are not functionally connected. Here, we present an analysis of synapses lacking RIM1α in autaptic cultured hippocampal neurons. This preparation allows ready access to presynaptic terminals and permits a detailed, quantitative analysis of presynaptic function. Such analyses cannot be performed in hippocampal slices or *C. elegans* neuromuscular junction but have been previously applied to Munc13-1$^{-/-}$ or Rab3A$^{-/-}$ synapses (Augustin et al., 1999; Geppert et al., 1997). Our results delineate the extent to which the properties of synapses lacking Munc13-1 or Rab3a overlap those of RIM1α$^{-/-}$ synapses and identify novel aspects of RIM1α function that are not shared by these interaction partners.

Results

RIM1α as a Priming Factor

Whole-cell recordings of autaptic neurons prepared from RIM1α$^{-/-}$ and littermate control mice showed that

*Correspondence: malenka@stanford.edu
[3]Present address: Department of Neuropathology, University of Bonn Medical Center, D53105 Bonn, Germany.

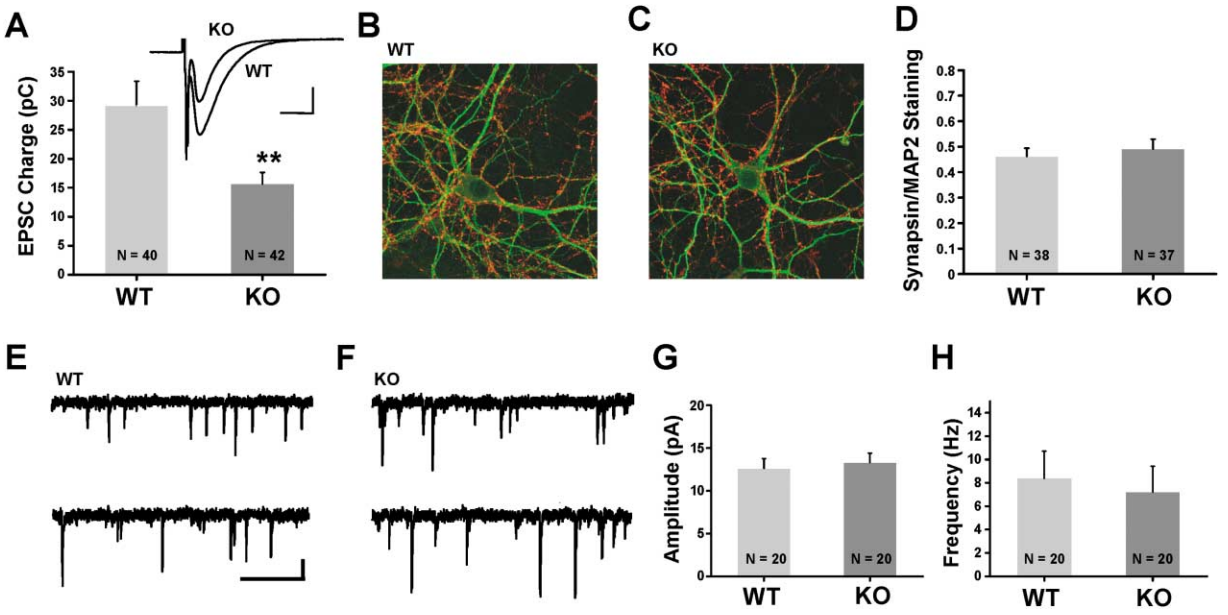

Figure 1. Synaptic Transmission Is Reduced in Rim1$\alpha^{-/-}$ Autapses

(A) EPSCs are reduced in RIM1$\alpha^{-/-}$ autapses (**$p < 0.005$). Inset shows representative traces (scale bars equal 10 ms/1 nA).

(B and C) Examples of immunostaining (red, Synapsin; green, MAP2).

(D) Average ratios of Synapsin/MAP2 staining (wt, 0.46 $\pm$ 0.03; KO, 0.49 $\pm$ 0.04, $p > 0.05$).

(E and F) Sample mEPSC recordings (scale bars equal 0.5 s/10 pA).

(G and H) Average amplitude and frequency of mEPSC events (wt, 12.62 $\pm$ 1.16 pA, 8.38 $\pm$ 2.33 Hz, n = 20 cells, 2590 events; KO, 13.31 $\pm$ 1.10 pA, 7.21 $\pm$ 2.21 Hz, n = 20 cells, 2816 events; $p > 0.05$).

RIM1$\alpha^{-/-}$ synapses exhibit a $\sim$50% reduction of the excitatory postsynaptic charge (wt, 29.1 $\pm$ 4.3 pC; KO, 15.7 $\pm$ 2.0 pC; $p < 0.005$; Figure 1A). This change could be due to a decrease in synapse numbers, a decline in postsynaptic receptor responsiveness, or a change in the synaptic release probability (P_r).

The interaction of RIM1α with α-Liprins (Schoch et al., 2002), which are implicated in synapse formation in invertebrates (Kaufmann et al., 2002; Zhen and Jin, 1999), suggests a role for RIM1α in synaptogenesis. We thus examined whether deletion of RIM1α alters total synapse numbers. Immunolabeling for the presynaptic protein Synapsin, however, showed no significant difference between RIM1$\alpha^{-/-}$ and wild-type synapses (Figures 1B–1D). We next examined postsynaptic responsiveness by recording miniature excitatory postsynaptic currents (mEPSCs), but we detected no difference in mEPSC amplitude (Figures 1E–1G). In addition, we found no difference in mEPSC frequency, a finding consistent with normal synapse numbers in RIM1$\alpha^{-/-}$ autapses (Figure 1H). Thus, synaptic responses in RIM1$\alpha^{-/-}$ neurons are likely reduced solely due to a decrease in P_r (Schoch et al., 2002).

RIM1α directly binds to Munc13-1, an active zone protein that is essential for synaptic vesicle priming (Augustin et al., 1999; Rosenmund et al., 2002), and is required for maintaining normal Munc13-1 levels (Schoch et al., 2002). We therefore next asked whether the decrease of synaptic strength in RIM1$\alpha^{-/-}$ synapses is due to a defect in priming, a biochemical event that is required subsequent to the ultrastructural appearance of docked vesicles in order for vesicles to be fusion competent and measurable in the "readily releasable pool" (RRP). To assay synaptic vesicle priming, we applied hypertonic sucrose and measured the resulting inward current (Rosenmund and Stevens, 1996), which in RIM1$\alpha^{-/-}$ autapses was $\sim$50% of the wild-type response (normalized wt, 1.0 $\pm$ 0.08; KO, 0.55 $\pm$ 0.05; $p < 0.005$; Figure 2A). This result suggests that the decrease in evoked EPSCs (Figure 1A) may be due to a corresponding decrease in the RRP (Figure 2A). To test whether additional abnormalities affecting Pr were present subsequent to priming, we calculated the vesicular release probability (P_{vr}). This measures the ratio of release evoked by an action potential to that evoked by hypertonic sucrose (Fernandez-Chacon et al., 2001). P_{vr} was not significantly different (Figure 2B). Thus, the synaptic vesicles remaining in the RRP of RIM1$\alpha^{-/-}$ synapses appear to exocytose normally in response to action potentials, and the decrease in synaptic responses in RIM1$\alpha^{-/-}$ autapses is attributable to the reduction in the RRP. Since another RIM protein, RIM2α, is expressed in the hippocampus (Wang et al., 2000), the remaining priming activity might be due to its presence. However, we did not detect RIM2α in wild-type or RIM1$\alpha^{-/-}$ cultures (Figure 2C), suggesting that RIM2α is not expressed at appreciable levels under our culture conditions.

The $\sim$50% decrease in the RRP in RIM1$\alpha^{-/-}$ synapses is similar to the $\sim$50% decrease in Munc13-1 levels in RIM1$\alpha^{-/-}$ mice (Schoch et al., 2002), suggesting that the two changes may be connected. Munc13-1 is a receptor for diacylglycerol and its stable analog, phorbol esters, which elicit an enhancement in transmitter re-

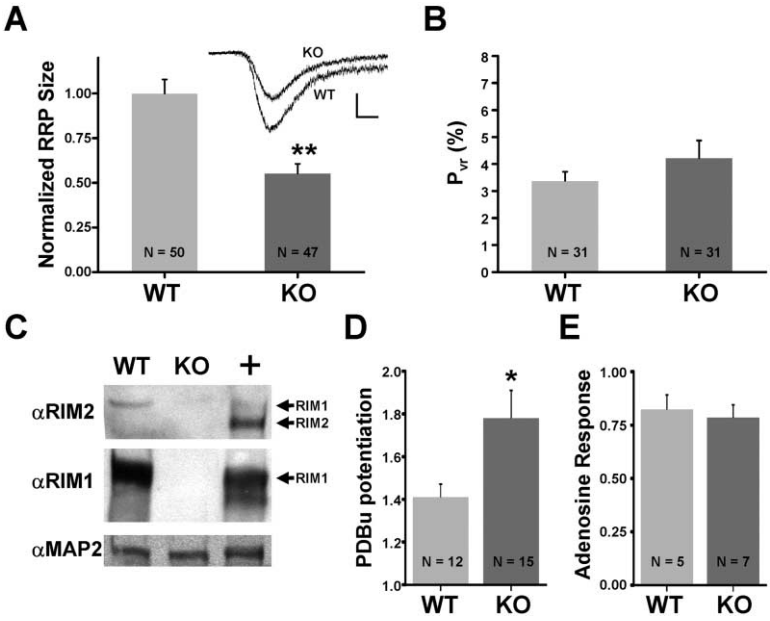

Figure 2. Defect in Synaptic Vesicle Priming in Rim1$\alpha^{-/-}$ Autapses

(A) Hypertonic sucrose-elicited RRP is decreased. Daily average wt response size was normalized to one for comparison. Inset shows sample traces (scale bars equal 1 s/0.5 nA; **$p < 0.005$).

(B) P_{vr} [(EPSC charge/RRP charge) $\times$ 100] is normal (wt, 3.38 $\pm$ 0.33; KO, 4.23 $\pm$ 0.69, $p > 0.05$).

(C) Western blot demonstrates absence of RIM2α in wild-type and RIM1$\alpha^{-/-}$ cultures. Due to similarity of the RIM1 and 2 proteins, there is a small amount of crossreactivity seen with the RIM2 antibody.

(D) Potentiation of EPSC amplitude by phorbol esters is augmented in RIM1$\alpha^{-/-}$ autapses (wt, 1.41 $\pm$ 0.06; KO, 1.78 $\pm$ 0.13, *$p < 0.05$).

(E) RIM1$\alpha^{-/-}$ autapses exhibit normal responses to inhibition by adenosine (wt, 0.83 $\pm$ 0.07; KO, 0.79 $\pm$ 0.06, $p > 0.05$).

lease because of binding to Munc13-1 (Betz et al., 1998; Rhee et al., 2002). Application of phorbol-12,13-dibutyrate (PDBu; 4 μM) to RIM1$\alpha^{-/-}$ autapses caused a 2-fold larger enhancement of EPSCs than in wild-type preparations (Figure 2D). This increase resembles that observed in Munc13-1$^{-/-}$ synapses (Rosenmund et al., 2002), supporting the hypothesis that the change in RRP in the RIM1$\alpha^{-/-}$ synapses is caused by a Munc13-1-dependent mechanism. To test whether other presynaptic regulatory events are altered in RIM1$\alpha^{-/-}$ synapses, we evaluated the effect of adenosine, which inhibits release by activating presynaptic A1 receptors. In contrast to the marked difference in the effects of PDBu, no difference in the inhibition of transmitter release by adenosine was detected (Figure 2E).

Short-Term Plasticity

To examine short-term plasticity in RIM1$\alpha^{-/-}$ synapses, we first measured the paired-pulse ratio. As observed in slices (Schoch et al., 2002), there was a relative change in this measure (Figures 3A–3C). Specifically, RIM1$\alpha^{-/-}$ autapses displayed less paired-pulse depression than wild-type autapses, with the largest effects occurring at the shortest interstimulus intervals. We next monitored the responses of RIM1α-deficient synapses to stimulus trains. Again as in hippocampal slices (Schoch et al., 2002), RIM1$\alpha^{-/-}$ synapses were better able to sustain responses during trains of high-frequency stimulation (Figures 3D–3F). In wild-type autapses, 14 Hz stimulation caused a ~50% decrease in the EPSC amplitude, but in RIM1$\alpha^{-/-}$ autapses, the EPSC was maintained near its initial value throughout. Plots of EPSC amplitudes during the trains revealed that wild-type and RIM1$\alpha^{-/-}$ EPSCs reached the same steady-state level (Figure 3F). Thus, despite the reduction in initial P_r in RIM1$\alpha^{-/-}$ autapses, at steady-state during high-frequency activity, P_r is not altered.

During high-frequency activity, the steady-state value of an EPSC is determined by the balance between supply and demand of vesicles and by changes in P_{vr} induced by the activity. Thus, activity-dependent differences in the RRP and/or the P_{vr} could account for the

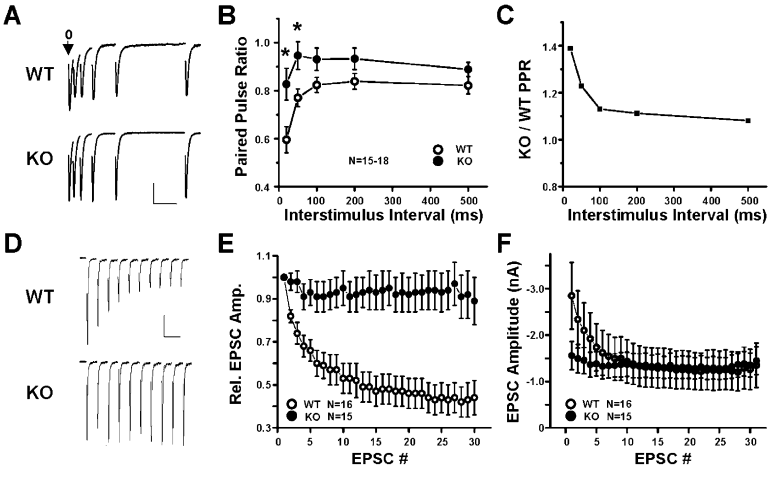

Figure 3. Deletion of RIM1α Alters Short-Term Plasticity

(A) Sample recordings from wt and RIM1$\alpha^{-/-}$ autapses in response to paired pulse stimulation. Arrow indicates first EPSC, with interstimulus intervals of 20, 50, 100, 200, 500 ms shown (scale bars equal 0.1 s/0.4 nA).

(B) Average paired pulse ratios (PPR) as a function of interstimulus interval (*$p < 0.05$).

(C) Ratio of average RIM1$\alpha^{-/-}$ to wt PPR.

(D) Sample recordings of the first 10 responses in a 14 Hz train (scale bars equal 0.1 s/0.4 nA).

(E) Average EPSC amplitudes during 14 Hz train normalized to size of first response.

(F) Steady-state absolute EPSC amplitudes converge to the same value in wt and RIM1$\alpha^{-/-}$ autapses during 14 Hz train.

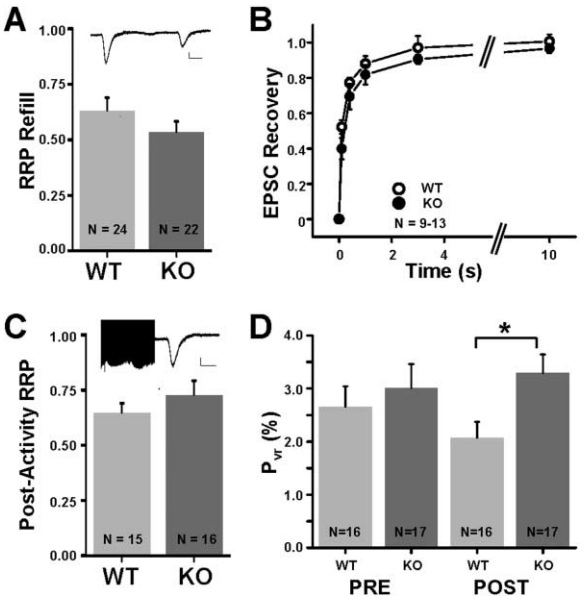

Figure 4. Activity-Dependent Changes in P_{vr} but not Vesicle Recycling Are Altered in Rim1$\alpha^{-/-}$ Autapses

(A) Basal rate of RRP refilling is normal. Average ratio of the second hypertonic sucrose response to the initial sucrose response measured 12 s prior. Inset shows sample recording (wt, 0.63 ± 0.05; KO, 0.54 ± 0.04; $p > 0.05$; scale bars equal 2 s/0.2 nA).

(B) Rate of EPSC recovery is normal after depletion of the RRP by activity. Graph shows ratio of test stimulus EPSC to initial EPSC as a function of time after RRP depletion.

(C) Relative amount of activity-dependent depletion of the RRP is normal in RIM1$\alpha^{-/-}$ autapses. The ratio of the hypertonic sucrose response immediately following a 14 Hz 100 stimuli train to the initial sucrose response (90 s prior) is shown. Inset shows sample recording with the train preceding the sucrose response (wt, 0.65 ± 0.04; KO, 0.73 ± 0.06; $p > 0.05$; scale bars equal 2 s/0.2 nA).

(D) Rim1$\alpha^{-/-}$ autapses exhibit a relative increase in P_{vr} during high-frequency activity. The "pre" P_{vr} value was obtained from the EPSC and sucrose response obtained 90 s prior to the stimulus train. The "post" P_{vr} was measured using the value of the last EPSC in a 14 Hz 100 stimuli train and the response to a sucrose pulse given immediately after the train (Pre P_{vr}: wt, 2.66 ± 0.38; KO, 3.01 ± 0.45; Post P_{vr}: wt, 2.07 ± 0.30; KO, 3.29 ± 0.35; *$p < 0.05$).

normalization of P_r during 14 Hz stimulation in RIM1$\alpha^{-/-}$ synapses. To examine this, we first measured the steady-state, activity-independent refilling rate of the RRP. The recovery of the RRP 12 s after it had been fully depleted by an initial pulse of hypertonic sucrose was similar in RIM1$\alpha^{-/-}$ and wild-type synapses (Figure 4A). This result also provides evidence that the defect in priming caused by the absence of RIM1α is not due to changes in the kinetics of priming, and thus it appears that RIM1α is, at least in part, responsible for determining the absolute size of the RRP.

Activity induces a Ca^{2+}-dependent acceleration of the refilling of the RRP (Zucker and Regehr, 2002). To test whether this process is enhanced by deletion of RIM1α, we examined the rate of recovery of the EPSC following depletion of the RRP by a 100 stimuli train at 40 Hz. We detected no abnormality in the recovery kinetics of the EPSC in RIM1$\alpha^{-/-}$ autapses (Figure 4B), indicating that the loss of RIM1α also does not affect the replenishment of synaptic vesicles under activity-stimulated conditions.

If, as the data thus far suggest, an increase in the size of the RRP does not underlie the normal steady-state 14 H_2 responses in RIM1$\alpha^{-/-}$ synapses, the relative loss of the RRP during the stimulus train should be similar between wild-type and RIM1$\alpha^{-/-}$ autapses. To evaluate this, we measured the initial RRP with a pulse of sucrose, applied a 100 stimuli train at 14 Hz 90 s later, and then immediately measured the RRP again (Figure 4C). The size of the RRP after the train relative to the initial RRP size was similar in the two preparations, indicating that the relative amount of activity-dependent refilling of the RRP was also similar. Thus, in RIM1$\alpha^{-/-}$ autapses, the RRP must still be ~50% of the RRP of wild-type autapses after the train. Since, at this time point, P_r is the same in wild-type and RIM1$\alpha^{-/-}$ autapses (i.e., the EPSC is the same size) and the P_r depends on the product of the P_{vr} and the RRP, the P_{vr} in the RIM1$\alpha^{-/-}$ synapses must have increased during the train. Indeed, calculation of P_{vr} at the beginning and end of the stimulus train revealed that while the initial P_{vr} was indistinguishable between the two genotypes, at the end of the stimulus train the P_{vr} was ~60% higher in RIM1$\alpha^{-/-}$ than in wild-type autapses (Figure 4D). Importantly, this property of RIM1$\alpha^{-/-}$ synapses is different from that observed in Munc13-1$^{-/-}$ autapses in which RRP size increases following a stimulus train (Rosenmund et al., 2002).

Ca^{2+} Responsiveness of RIM1$\alpha^{-/-}$ Synapses

Several observations suggest that the Ca^{2+} dependence of release may be abnormal in RIM1$\alpha^{-/-}$ synapses. In vitro, RIM1α exhibits Ca^{2+}-dependent binding to synaptotagmin 1 (Coppola et al., 2001; Schoch et al., 2002) and also contains C_2 domains that function as Ca^{2+}/phospholipid binding modules (although critical residues for Ca^{2+} binding are missing) (Wang et al., 1997). Moreover, an interaction between Ca^{2+} channels and RIM-BPs has been described (Hibino et al., 2002). Finally, Munc13-1 also contains C_2 domains (Brose et al., 1995). To investigate the Ca^{2+} responsiveness of RIM1$\alpha^{-/-}$ synapses, we varied external Ca^{2+} and Mg^{2+} concentrations from 1 to 8 mM and 8 to 1 mM, respectively, and normalized EPSC size to that obtained in 4 mM Ca^{2+}. Using this protocol, we observed no difference between RIM1$\alpha^{-/-}$ and wild-type autapses (Figure 5A).

Ca^{2+}-dependent neurotransmitter release can be divided into two components, termed "synchronous" and "asynchronous" release, that can be evaluated by examining the kinetic components of EPSCs (Stevens, 2003). As the relative amount of asynchronous release may influence synaptic responses during high-frequency stimulation (Hagler and Goda, 2001; Lu and Trussell, 2000), we compared the kinetic components of wild-type and RIM1$\alpha^{-/-}$ EPSCs by fitting the integral of each cell's EPSC to a double exponential equation. While the decay time constant for the synchronous (fast) component of release was not affected by deletion of RIM1α, the decay time constant for asynchronous (slow) release was ~3 times faster (synchronous τ: wt, 6.3 ± 0.6 ms; KO, 6.2 ± 0.5 ms; $p > 0.05$; asynchronous τ: wt, 174 ± 22 ms; KO, 50 ± 7 ms, $p < 0.005$; Figures 5B and 5C). Evaluating the relative contribution of each kinetic component to the EPSC within a cell revealed a ~50% de-

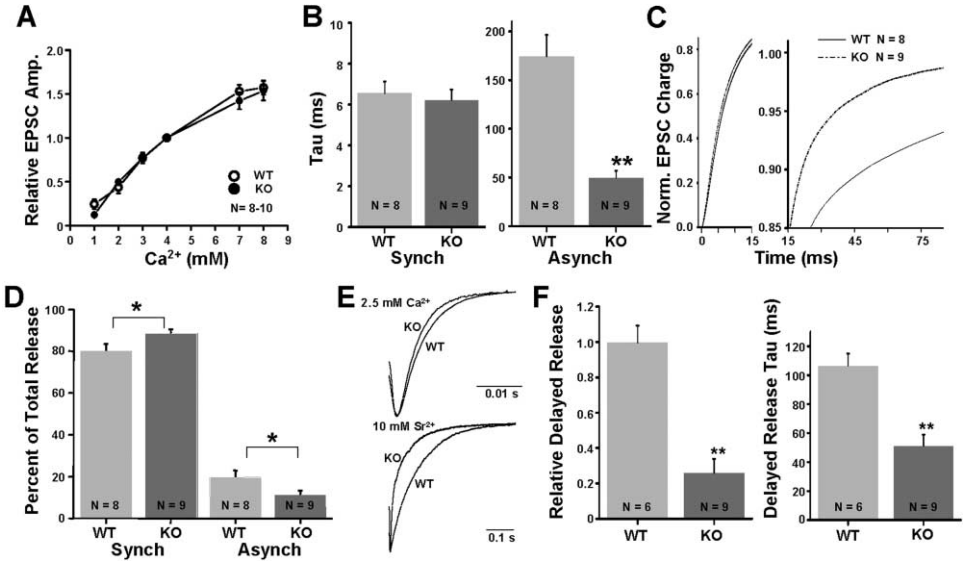

Figure 5. Calcium Dependence of Release Is Normal but Asynchronous Release Is Altered in Rim1α$^{-/-}$ Autapses

(A) Dependence of EPSC amplitude on external calcium concentration in wt and RIM1α$^{-/-}$ autapses. Amplitudes were normalized to response at 4 mM Ca^{2+}/4 mM Mg^{2+}, which was perfused prior to each test concentration so that error due to rundown was avoided (n = 8–10 cells per data point except for KO at 1 mM Ca^{2+} n = 2, p > 0.05).

(B) Decay time constant for asynchronous, but not synchronous, release is faster in RIM1α$^{-/-}$ autapses (**p < 0.005).

(C) Average of normalized EPSC integrals illustrating decay during early (left) and late (right) periods.

(D) Asynchronous release is half of the normal percentage of total release per neuron in RIM1α$^{-/-}$ autapses (Synchronous: wt, 80.2 ± 3.2; KO, 88.6 ± 1.9; Asynchronous: wt, 19.7 ± 3.2; KO, 11.4 ± 1.9; *p < 0.05).

(E) Average of normalized EPSC traces in 2.5 mM calcium and in 10 mM strontium. Note time scale difference.

(F) Strontium-mediated delayed release charge and decay time constant are decreased in RIM1α$^{-/-}$ autapses (**p < 0.005).

crease in the amount of asynchronous release in RIM1α$^{-/-}$ autapses (Figure 5D). Further, the average total amount of synchronous release in RIM1α$^{-/-}$ autapses across all cells was 63% of wild-type, while the average amount of asynchronous release was 38%, again indicating a preferential loss of the asynchronous component.

If RIM1α preferentially affects the asynchronous component of release, performing a manipulation that augments this component of release should amplify the differences between RIM1α$^{-/-}$ and wild-type autapses. To do this, we examined EPSCs evoked in 10 mM strontium (Figures 5E and 5F), a manipulation that greatly augments the asynchronous release component (Xu-Friedman and Regehr, 2000). Averages of scaled EPSCs from RIM1α$^{-/-}$ and wild-type autapses show the expected larger difference in asynchronous release when EPSCs were evoked in strontium rather than Ca^{2+} (Figure 5E). In strontium, EPSCs from RIM1α$^{-/-}$ autapses had 26% of the average delayed release and decayed about twice as fast as EPSCs from wild-type autapses (relative delayed strontium release: wt, 1.0 ± 0.09; KO, 0.26 ± 0.08; p < 0.005; delayed strontium release τ: wt, 107 ± 8.2 ms; KO, 51 ± 7.7; p < 0.005). These data provide independent confirmation and thus further support for an important role of RIM1α in the control of asynchronous release.

Discussion

The active zone is composed of a multiprotein complex that includes RIM1α as a major component. RIM1α interacts directly or indirectly with most other known active zone proteins, is essential for normal neurotransmitter release, and is regulated by phosphorylation. We have examined the properties of mammalian synapses lacking RIM1α by analyzing synaptic transmission in autaptic cultures of hippocampal neurons, a preparation that permits a detailed characterization of presynaptic function. We have also taken advantage of the fact that neurons lacking Munc13-1 or Rab3A, two major binding partners of RIM1α, were previously analyzed in the same manner (Augustin et al., 1999; Geppert et al., 1997; Rosenmund et al., 2002; Schlüter et al., 2004).

Our findings suggest that RIM1α shapes three properties of transmitter release. (1) RIM1α enhances transmitter release by potentiating the amount but not the kinetics of synaptic vesicle priming. This function of RIM1α accounts for ~50% of the RRP of synaptic vesicles in hippocampal synapses. The remaining ~50% of the RRP is likely independent of RIMs because RIM2α, the only other full-length RIM isoform (Wang and Sudhof, 2003), was undetectable in the cultured neurons. (2) RIM1α contributes to the regulation of STP. This appears, at least in part, to be due to an activity-dependent change in the vesicular release probability (P_{vr}). (3) RIM1α is essential for normal asynchronous Ca^{2+}-triggered release. In the absence of RIM1α, the relative contribution of asynchronous release to total release is decreased by ~50%, and asynchronous release kinetics are accelerated. Importantly, RIM1α is not required for synaptogenesis, normal quantal size, normal spontaneous release, the synchronous component of evoked release, or the activity-independent and -dependent com-

ponents of refilling of the primed pool of synaptic vesicles.

This more detailed analysis of presynaptic function in autapses complements and extends prior studies on RIM1α (Betz et al., 2001; Castillo et al., 2002; Koushika et al., 2001; Schoch et al., 2002; Sun et al., 2002) and its interacting partners, Rab3A (Castillo et al., 1997; Geppert et al., 1997; Schoch et al., 2002) and Munc13-1 (Aravamudan et al., 1999; Augustin et al., 1999; Betz et al., 1998; Rosenmund et al., 2002). Our results suggest that RIM1α functions as a modulator of release that operates both during priming (as evidenced by the decrease of the RRP) and Ca^{2+} triggering (as evidenced by the change in asynchronous release and the increased P_{vr} during repetitive stimulation). The dual activity of RIM1α in both priming and Ca^{2+} triggering of release mirrors its dual interaction with Munc13-1 and Rab3A, suggesting a potential sequential interaction.

Several lines of evidence suggest that the ~50% decrease in synaptic responses in the RIM1α$^{-/-}$ synapses is caused by the loss of the RIM1α/Munc13-1 interaction. (1) Similar to their effect on Munc13-1-deficient synapses (Rosenmund et al., 2002), phorbol esters, which act in large part by binding to Munc13-1 (Rhee et al., 2002), caused a relatively larger enhancement of release in RIM1α$^{-/-}$ synapses than in control synapses. (2) Overexpression of the domain of Munc13-1 that binds to RIM1α also caused a ~50% decrease in the RRP (Betz et al., 2001). Conversely, truncated Munc13-1 that is unable to bind to RIM1α rescued only ~50% of the RRP in Munc13-1 deficient synapses, while full-length Munc13-1 rescued ~100% of the RRP (Betz et al., 2001). (3) In *C. elegans*, a mutant form of Syntaxin 1 with a constitutively "open" conformation compensates for the defects in both the RIM and Munc13 genes (Koushika et al., 2001; Richmond et al., 2001), suggesting that the RIM1α/Munc13-1 complex operates in the same pathway that acts on SNARE complex assembly during priming. Taken together, these data suggest that the interaction of RIM1α with Munc13-1 is a central component of the priming machinery, although other interactions of RIM1α, e.g., binding to SNAP-25 (Coppola et al., 2001), may also contribute.

Although the loss of the RIM1α/Munc13-1 interaction in RIM1α$^{-/-}$ synapses likely accounts for the decrease in the RRP due to a priming defect, it is unlikely to also completely explain the observed abnormalities in STP. First, the increase in paired-pulse ratios in the RIM1α$^{-/-}$ synapses is very similar to the changes observed in Rab3A$^{-/-}$ synapses that exhibited no change in P_r (Geppert et al., 1997; Schoch et al., 2002). Second, in GABAergic RIM1α$^{-/-}$ synapses, paired-pulse responses are altered (Schoch et al., 2002) even though inhibitory synapses do not require Munc13-1, presumably because Munc13-2 substitutes for Munc13-1 (Augustin et al., 1999; Rosenmund et al., 2002). Importantly, the brain form of Munc13-2 does not bind to RIM1α (Brose et al., 1995). This suggests that the STP phenotype in inhibitory synapses, and by extension in all synapses, is independent of Munc13-1. Although we cannot rule out that the decreased P_r in RIM1α$^{-/-}$ synapses contributes to the increase in paired-pulse responses (Zucker and Regehr, 2002), decreased P_r cannot explain the similar increase in paired-pulse responses in Rab3A$^{-/-}$ mice and the activity-dependent increase in P_{vr} in the RIM1α$^{-/-}$ mice.

A particularly unexpected observation was that RIM1α$^{-/-}$ synapses displayed a selective change in asynchronous release that was not detected in Munc13-1$^{-/-}$ synapses (Augustin et al., 1999; Rosenmund et al., 2002). While the molecular mechanisms underlying synchronous release are relatively well understood, to our knowledge these results provide one of the first links of any synaptic protein to the poorly understood processes controlling asynchronous release. One speculative model is that normally vesicles pass through successive "priming," "asynchronous," and "synchronous" stages, and that for each stage a defined number of "slots" is available. If this idea is correct, in the RIM1α-deficient synapses the number of slots available for priming is decreased, but the number of downstream slots does not change. This might lead to a faster transition between the stages. However, alternative models are possible, and a better definition of the nature of asynchronous release and the identity of the Ca^{2+} sensor involved will be required before these models can be tested.

In summary, using RIM1α$^{-/-}$ autapses, we have demonstrated that RIM1α normally enhances P_r by increasing the size of the RRP but does not affect the rate of vesicle priming at rest or after stimulation. Deletion of RIM1α also provided evidence that RIM1α plays an important role in the regulation of P_{vr} during trains of activity and the kinetics of asynchronous release. These data support the notion that RIM1α is a key regulator of vesicle maturation at the active zone, from priming to Ca^{2+} triggering of synaptic vesicle fusion. Regulation of these late stages of neurotransmitter release is a likely mechanism explaining RIM1α's role in forms of short- and long-term synaptic plasticity.

Experimental Procedures

Cell Culture

Autaptic cultures were prepared by plating mechanically dissociated hippocampal CA1-CA3 neurons from P0–P1 RIM1α$^{-/-}$ mice (Schoch et al., 2002) and littermate wild-type controls at 1000 cells/cm^2 onto glial-covered PDL/collagen-treated microislands and grown in Neurobasal-A media supplemented with 4% B-27 and 2 mM Glutamax-1 (GIBCO) for 12–15 days (Bekkers and Stevens, 1991). Rat glia were plated at 2000 cells/cm^2 for 3–7 days prior to neuronal plating (Noble and Mayer-Proschel, 1998).

Electrophysiology

Whole-cell recordings were performed on in vitro days (DIV) 12–15 using an Axopatch-1D amplifier (Axon Instruments) at room temperature. External solution consisted of (in mM): 115 NaCl, 23 glucose, 26 sucrose, 5 HEPES, 5 KCl, 2.5 $CaCl_2$, 1.3 $MgSO_4$, 0.05 picrotoxin, and 0.05 D-AP5 (Tocris). Internal pipette recording solution consisted of (in mM): 110 K-methanesulfonate, 5 $MgCl_2$, 10 NaCl, 40 HEPES, 0.6 EGTA, 2 MgATP, 0.3 Na_3GTP. Cells were voltage-clamped at −70 mV except for 1 ms depolarizations to 0 mV to elicit action potentials. Data were filtered at 1–2 kHz and acquired at 2–5 kHz using Igor software (Wavemetrics). Recordings and data analysis were performed blinded to the genotype of the sample. All chemicals were obtained from Sigma unless specifically noted otherwise. Miniature EPSC analysis was performed manually using Synaptosoft software with an amplitude threshold of 5 pA. All solution changes were made using a rapid microperfusion device (SF-77B, Warner Instruments). RRP was elicited by perfusion of 0.5 M sucrose in external solution for 4 s. To quantify effects of phorbol-12,13-dibutyrate (4 μM, Calbiochem) and N^6-cyclopentyladenosine

(50 μM), average EPSC amplitude (90 s period) 60 s after drug perfusion started was compared to average EPSC amplitude (90 s period) immediately prior to drug application. No correction for EPSC rundown was made.

Immunocytochemistry and Immunoblotting

Hippocampal cultures of 12–14 DIV were used for immunocytochemistry and immunoblotting according to standard procedures (see Supplemental Data at http://www.neuron.org/cgi/content/full/42/6/889/DC1 for details).

Kinetic Analysis of EPSC

Decay time constants (τ, tau) and absolute amounts of release were calculated under basal conditions by fitting the integral of the EPSC (average of 3 consecutive EPSCs from each cell) to the double exponential equation, $y = y_0 + A_1e^{(-x/t_1)} + A_2e^{(-x/t_2)}$ and in strontium, by fitting the normalized average EPSCs during the delayed release phase (from 10 ms after the onset of the EPSC to its return to baseline, 400–600 ms later) to the single exponential equation, $y = y_0 + Ae^{(-x/t)}$ using Microcal Origin 6.1 software (t_1 = synchronous τ, t_2 = asynchronous τ, A_1 = amount of synchronous release component, A_2 = amount of asynchronous release component). The R^2 values for all fits were greater than 0.999.

Statistical Analysis

All error bars indicate the standard error of the mean (SEM). All results are reported as ± SEM. p values were calculated using two-tailed Student's t test.

Acknowledgments

This work was supported by NIH grants MH63394 (R.C.M.) and NS41344 (N.C.) and HHMI (T.C.S., N.C.). We thank members of the Malenka lab and J. Dittman for insightful discussions; Tina Lizama, Liz Saura, Jerron Fisher, and Melissa Pak for outstanding technical assistance; C. Rosenmund and J. Sullivan for advice regarding autaptic cultures; and N. Hamlin and A. Roth for mouse husbandry and genotyping.

Received: January 27, 2004
Revised: April 7, 2004
Accepted: May 17, 2004
Published: June 23, 2004

References

Aravamudan, B., Fergestad, T., Davis, W.S., Rodesch, C.K., and Broadie, K. (1999). *Drosophila* UNC-13 is essential for synaptic transmission. Nat. Neurosci. *2*, 965–971.

Augustin, I., Rosenmund, C., Sudhof, T.C., and Brose, N. (1999). Munc13–1 is essential for fusion competence of glutamatergic synaptic vesicles. Nature *400*, 457–461.

Bekkers, J.M., and Stevens, C.F. (1991). Excitatory and inhibitory autaptic currents in isolated hippocampal neurons maintained in cell culture. Proc. Natl. Acad. Sci. USA *88*, 7834–7838.

Betz, A., Ashery, U., Rickmann, M., Augustin, I., Neher, E., Sudhof, T.C., Rettig, J., and Brose, N. (1998). Munc13–1 is a presynaptic phorbol ester receptor that enhances neurotransmitter release. Neuron *21*, 123–136.

Betz, A., Thakur, P., Junge, H.J., Ashery, U., Rhee, J.S., Scheuss, V., Rosenmund, C., Rettig, J., and Brose, N. (2001). Functional interaction of the active zone proteins Munc13–1 and RIM1 in synaptic vesicle priming. Neuron *30*, 183–196.

Brose, N., Hofmann, K., Hata, Y., and Sudhof, T.C. (1995). Mammalian homologues of *Caenorhabditis elegans* unc-13 gene define novel family of C2-domain proteins. J. Biol. Chem. *270*, 25273–25280.

Castillo, P.E., Janz, R., Sudhof, T.C., Tzounopoulos, T., Malenka, R.C., and Nicoll, R.A. (1997). Rab3A is essential for mossy fibre long-term potentiation in the hippocampus. Nature *388*, 590–593.

Castillo, P.E., Schoch, S., Schmitz, F., Sudhof, T.C., and Malenka, R.C. (2002). RIM1alpha is required for presynaptic long-term potentiation. Nature *415*, 327–330.

Coppola, T., Magnin-Luthi, S., Perret-Menoud, V., Gattesco, S., Schiavo, G., and Regazzi, R. (2001). Direct interaction of the Rab3 effector RIM with Ca^{2+} channels, SNAP-25, and synaptotagmin. J. Biol. Chem. *276*, 32756–32762.

Fernandez-Chacon, R., Konigstorfer, A., Gerber, S.H., Garcia, J., Matos, M.F., Stevens, C.F., Brose, N., Rizo, J., Rosenmund, C., and Sudhof, T.C. (2001). Synaptotagmin I functions as a calcium regulator of release probability. Nature *410*, 41–49.

Geppert, M., Goda, Y., Stevens, C.F., and Sudhof, T.C. (1997). The small GTP-binding protein Rab3A regulates a late step in synaptic vesicle fusion. Nature *387*, 810–814.

Hagler, D.J., Jr., and Goda, Y. (2001). Properties of synchronous and asynchronous release during pulse train depression in cultured hippocampal neurons. J. Neurophysiol. *85*, 2324–2334.

Hibino, H., Pironkova, R., Onwumere, O., Vologodskaia, M., Hudspeth, A.J., and Lesage, F. (2002). RIM binding proteins (RBPs) couple Rab3-interacting molecules (RIMs) to voltage-gated Ca(2+) channels. Neuron *34*, 411–423.

Kaufmann, N., DeProto, J., Ranjan, R., Wan, H., and Van Vactor, D. (2002). *Drosophila* liprin-alpha and the receptor phosphatase Dlar control synapse morphogenesis. Neuron *34*, 27–38.

Ko, J., Na, M., Kim, S., Lee, J.R., and Kim, E. (2003). Interaction of the ERC family of RIM-binding proteins with the Liprin-{alpha} family of multidomain proteins. J. Biol. Chem. *278*, 42377–42385.

Koushika, S.P., Richmond, J.E., Hadwiger, G., Weimer, R.M., Jorgensen, E.M., and Nonet, M.L. (2001). A post-docking role for active zone protein Rim. Nat. Neurosci. *4*, 997–1005.

Lu, T., and Trussell, L.O. (2000). Inhibitory transmission mediated by asynchronous transmitter release. Neuron *26*, 683–694.

Noble, M., and Mayer-Proschel, M. (1998). Culture of astrocytes, oligodendrocytes, and O-2A progenitor cells. In Culturing Nerve Cells, G. Banker and K. Goslin, eds. (Cambridge, MA: MIT Press), pp. 526–529.

Ohtsuka, T., Takao-Rikitsu, E., Inoue, E., Inoue, M., Takeuchi, M., Matsubara, K., Deguchi-Tawarada, M., Satoh, K., Morimoto, K., Nakanishi, H., and Takai, Y. (2002). Cast: a novel protein of the cytomatrix at the active zone of synapses that forms a ternary complex with RIM1 and munc13–1. J. Cell Biol. *158*, 577–590.

Ozaki, N., Shibasaki, T., Kashima, Y., Miki, T., Takahashi, K., Ueno, H., Sunaga, Y., Yano, H., Matsuura, Y., Iwanaga, T., et al. (2000). cAMP-GEFII is a direct target of cAMP in regulated exocytosis. Nat. Cell Biol. *2*, 805–811.

Rhee, J.S., Betz, A., Pyott, S., Reim, K., Varoqueaux, F., Augustin, I., Hesse, D., Sudhof, T.C., Takahashi, M., Rosenmund, C., and Brose, N. (2002). Beta phorbol ester- and diacylglycerol-induced augmentation of transmitter release is mediated by Munc13s and not by PKCs. Cell *108*, 121–133.

Richmond, J.E., Weimer, R.M., and Jorgensen, E.M. (2001). An open form of syntaxin bypasses the requirement for UNC-13 in vesicle priming. Nature *412*, 338–341.

Rosenmund, C., and Stevens, C.F. (1996). Definition of the readily releasable pool of vesicles at hippocampal synapses. Neuron *16*, 1197–1207.

Rosenmund, C., Sigler, A., Augustin, I., Reim, K., Brose, N., and Rhee, J.S. (2002). Differential control of vesicle priming and short-term plasticity by Munc13 isoforms. Neuron *33*, 411–424.

Schlüter, O., Schmitz, F., Jahn, R., Rosenmund, C., and Südhof, T.C. (2004). A complete genetic analysis of neuronal Rab3 function. J. Neurosci., in press.

Schoch, S., Castillo, P.E., Jo, T., Mukherjee, K., Geppert, M., Wang, Y., Schmitz, F., Malenka, R.C., and Sudhof, T.C. (2002). RIM1alpha forms a protein scaffold for regulating neurotransmitter release at the active zone. Nature *415*, 321–326.

Stevens, C.F. (2003). Neurotransmitter release at central synapses. Neuron *40*, 381–388.

Sun, L., Bittner, M.A., and Holz, R.W. (2002). Rim and exocytosis:

Rab3a-binding and secretion-enhancing domains are separate and function independently. Ann. N Y Acad. Sci. *971*, 244–247.

Sun, L., Bittner, M.A., and Holz, R.W. (2003). Rim, a component of the presynaptic active zone and modulator of exocytosis, binds 14–3-3 through its N terminus. J. Biol. Chem. *278*, 38301–38309.

Wang, Y., and Sudhof, T.C. (2003). Genomic definition of RIM proteins: evolutionary amplification of a family of synaptic regulatory proteins. Genomics *81*, 126–137.

Wang, Y., Okamoto, M., Schmitz, F., Hofmann, K., and Sudhof, T.C. (1997). Rim is a putative Rab3 effector in regulating synaptic-vesicle fusion. Nature *388*, 593–598.

Wang, Y., Sugita, S., and Sudhof, T.C. (2000). The RIM/NIM family of neuronal C2 domain proteins. Interactions with Rab3 and a new class of Src homology 3 domain proteins. J. Biol. Chem. *275*, 20033–20044.

Wang, X., Hu, B., Zimmermann, B., and Kilimann, M.W. (2001). Rim1 and rabphilin-3 bind Rab3-GTP by composite determinants partially related through N-terminal alpha-helix motifs. J. Biol. Chem. *276*, 32480–32488.

Wang, Y., Liu, X., Biederer, T., and Sudhof, T.C. (2002). A family of RIM-binding proteins regulated by alternative splicing: implications for the genesis of synaptic active zones. Proc. Natl. Acad. Sci. USA *99*, 14464–14469.

Xu-Friedman, M.A., and Regehr, W.G. (2000). Probing fundamental aspects of synaptic transmission with strontium. J. Neurosci. *20*, 4414–4422.

Zhen, M., and Jin, Y. (1999). The liprin protein SYD-2 regulates the differentiation of presynaptic termini in *C. elegans*. Nature *401*, 371–375.

Zucker, R.S., and Regehr, W.G. (2002). Short-term synaptic plasticity. Annu. Rev. Physiol. *64*, 355–405.